Robust Estimation and Detection Schemes in non-Standard Conditions for Radar, Array Processing and Imaging

Jean-Philippe Ovarlez

ONERA, The French Aerospace Lab,
Département ElectroMagnétisme et Radar,
Unité *Méthodes Avancées en Traitement de Signal*
& Laboratoire SONDRA de CentraleSupélec

20 novembre 2019

ONERA

THE FRENCH AEROSPACE LAB

Plan

Plan

1. Introduction
   - Introduction
   - Radar and Imaging Sensors - New challenges
   - Applicative Context
   - Methodological Context
2. Some Background on Detection Theory
3. Robust Estimation and Detection
4. Applications and Results in Radar, STAP, SAR imaging, Hyperspectral Imaging

Radar Detection

RADAR = RAdio Detection And Ranging



- emits and receives electromagnetic waves,
- detects the presence of targets,

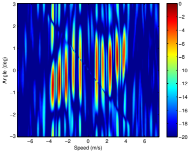

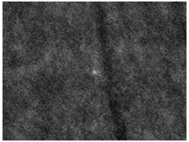

Cartes de détection

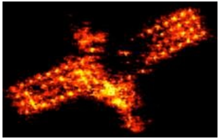

Image ISAR

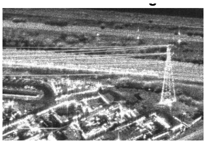

Image SAR

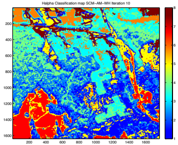

Classification SAR

- but also: estimates parameters (range, radial velocity, angles of presentation, acceleration, amplitude (related to Radar Cross Section), etc.),
- images, classifies, recognizes.

> Note : Almost all the conventional Statistical Signal Processing methodologies and background modelling tools are based on Gaussian hypothesis (**standard conditions**).

Radar and Imaging Sensors - New challenges

Positioning: facing the new non-standard conditions

- **Complex Environments**: ground, dynamic environments (sea, ionosphere), heterogeneous, non-Gaussian, reverberating.
- **Complex targets**: small RCS, extended targets, fluctuating, dispersive, anisotropic.
- **Sensor Diversity**: temporal, spatial, polarimetric, interferometric, spectral.
- **Improvement of sensor resolution**: spatial, spectral, angular.
- **Outliers, jamming**
- **Increase of the dimension and the size of signals to analyze.**

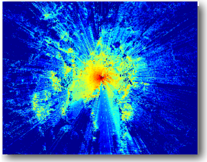

Heterogeneous Environments

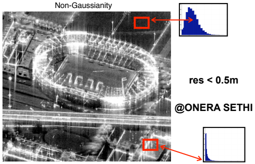

Non-Gaussian Environments

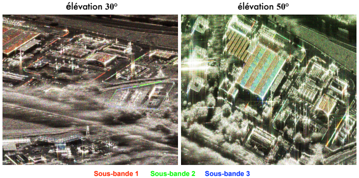

Non-Stationary Targets and Environments

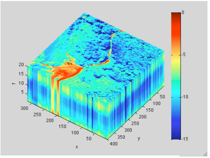

Curse of Dimensionality

Applicative Context

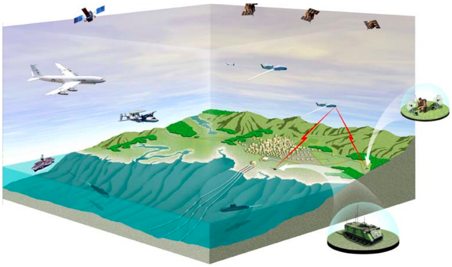

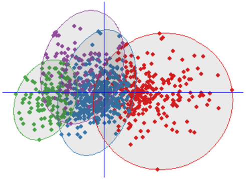

Finance
- Time Series
- Portofolio Optimization
- Risk Management
- Classification
- Prediction

Air, ground, sea Surveillance
- Radar Detection, Space-Time Adaptive Processing
- Synthetic Aperture Radar
- Sources Localization
- Interferometric, Polarimetric Classification
- Change Detection, Infrastructure Monitoring
- Anomaly Detection in Hyperspectral Imaging
- MIMO Radar
- Tracking

Big Data
- Recognition
- Classification, Clustering
- Dimension Reduction
- Machine Learning, Deep Learning
- Graphs Analysis
- Learning Techniques

Methodological Context

Goals: Improvement of sensors performance and their processing

- To model thanks **statistics** the variability of the unknown environment and data,
- To estimate the **spectral properties** of the environment (ionosphere, sea, wind through forest, etc.),
- To elaborate **estimators** and **detectors** that are *robust* and *adaptive* to these environments,
- To **regulate the False Alarm** on these *heterogeneous*, *non-stationary*, *non-Gaussian* environments,
- To **improve** the classification, the clustering techniques.

Methods: Statistical Signal Processing

- **Robust Estimation Techniques** of spectral and statistic characteristics of the environment and targets: adaptivity, statistic learning, cognitive, maximal exploitation of the *a priori*,
- **Optimal Detection Schemes** (Likelihood, Bayesian) for stealthy target embedded in these complex environments,
- Exploitation of emerging statistical Signal Processing techniques: Time-Frequency Analysis, Random Matrix Theory, Clustering, Compressive Sensing, etc.

Special issue: *Greco et al.*, Introduction to the Issue on Advanced Signal Processing Techniques for Radar Applications, IEEE Journal of Selected Topics in Signal Processing, 2015.
Book: *Greco and De Maio*, *Modern Radar Detection Theory*, Scitech Publishing, IET, 2015.

Methodological Context

Goals: Improvement of sensors performance and their processing

- To model thanks **statistics** the variability of the unknown environment and data,
- To estimate the **spectral properties** of the environment (ionosphere, sea, wind through forest, etc.),
- To elaborate **estimators** and **detectors** that are *robust* and *adaptive* to these environments,
- To **regulate the False Alarm** on these *heterogeneous*, *non-stationary*, *non-Gaussian* environments,
- To **improve** the classification, the clustering techniques.

Methods: Statistical Signal Processing

- **Robust Estimation Techniques** of spectral and statistic characteristics of the environment and targets: adaptivity, statistic learning, cognitive, maximal exploitation of the *a priori*,
- **Optimal Detection Schemes** (Likelihood, Bayesian) for stealthy target embedded in these complex environments,
- Exploitation of emerging statistical Signal Processing techniques: Time-Frequency Analysis, Random Matrix Theory, Clustering, Compressive Sensing, etc.

Special issue: *Greco et al.*, Introduction to the Issue on Advanced Signal Processing Techniques for Radar Applications, IEEE Journal of Selected Topics in Signal Processing, 2015.
Book: *Greco and De Maio*, *Modern Radar Detection Theory*, Scitech Publishing, IET, 2015.

Plan

1. Introduction

2. Some Background on Detection Theory
   - Problem Statement
   - Modeling Homogeneous Gaussian Noise/Clutter
   - Examples of CFAR Detection Schemes Under Gaussian Noise
   - Examples of Gaussian Hypothesis Failure

3. Robust Estimation and Detection

4. Applications and Results in Radar, STAP, SAR imaging, Hyperspectral Imaging

Problem Statement

- In a m-vector $\mathbf{z}$, detecting an unknown complex deterministic signal $\mathbf{s} = A\,\mathbf{p}$ embedded in an additive noise $\mathbf{y}$ can be written as the following statistical test:

$$\begin{cases} \text{Hypothesis } H_0: & \mathbf{z} = \mathbf{y} & \mathbf{z}_i = \mathbf{y}_i & i = 1, \dots, n \\ \text{Hypothesis } H_1: & \mathbf{z} = \mathbf{s} + \mathbf{y} & \mathbf{z}_i = \mathbf{y}_i & i = 1, \dots, n \end{cases}$$

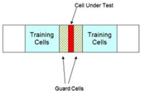

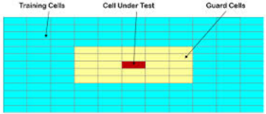

where the $\mathbf{z}_i$'s are n "signal-free" independent secondary data used to estimate the noise parameters. $\Rightarrow$ Neyman-Pearson criterion *[Kay 93]*

- Detection test: comparison between the Likelihood Ratio $\Lambda(\mathbf{z})$ and a detection threshold λ:

$$\Lambda(\mathbf{z}) = \frac{p_{\mathbf{z}}(\mathbf{z}/H_1)}{p_{\mathbf{z}}(\mathbf{z}/H_0)} \underset{H_0}{\overset{H_1}{\gtrless}} \lambda\,,$$

- Probability of False Alarm (type-I error): $P_{fa} = \mathbb{P}(\Lambda(\mathbf{z}) > \lambda/H_0)$
- Probability of Detection: $P_d = \mathbb{P}(\Lambda(\mathbf{z}) > \lambda/H_1)$ for different Signal-to-Noise Ratios (SNR),
- When P_{fa} does not depend on the noise/clutter parameters, the detector is said to be **CFAR (Constant False Alarm Rate)**.

Modeling Homogeneous Gaussian Noise/Clutter

Problem to solve in Gaussian environment

$$\begin{cases} H_0: & \mathbf{z} = \mathbf{y} & \mathbf{z}_i = \mathbf{y}_i & i = 1, \dots, n \\ H_1: & \mathbf{z} = \mathbf{s} + \mathbf{y} & \mathbf{z}_i = \mathbf{y}_i & i = 1, \dots, n \end{cases}$$

where $\mathbf{y}$ and $\mathbf{y}_i \sim \mathcal{CN}(\mathbf{0}_m, \mathbf{\Sigma})$, i.e. $p_{\mathbf{z}}(\mathbf{z}) = \dfrac{1}{\pi^m \, |\mathbf{\Sigma}|} \exp\left(-\mathbf{z}^H \, \mathbf{\Sigma}^{-1} \, \mathbf{z}\right)$

Goal: to choose the best hypothesis while minimizing the risk of being wrong (False Alarm) from an observation vector $\mathbf{z}$

$\Longrightarrow$ **All is known for Gaussian assumption!**

Sample Covariance Matrix (SCM)

When $\mathbf{\Sigma}$ is unknown, the Gaussian environment is modeled through the SCM:

$$\hat{\mathbf{S}}_n = \frac{1}{n} \sum_{i=1}^{n} \mathbf{z}_i \, \mathbf{z}_i^H \, .$$

- Simple Covariance Matrix estimator, Very tractable,
- Wishart distributed, Well-known statistical properties: unbiased and efficient.
- The SCM is the most likely covariance matrix estimate (MLE) and is the empirical mean of the cross-correlation of n m-vectors $\mathbf{z}_i$ where n can represent any samples support (range, time, spatial, angular domain)

Examples of CFAR Detection Schemes Under Gaussian Noise

- Adaptive Matched Filter *[Robey et al. 92]*: $\Lambda_{AMF}(\mathbf{z}) = \dfrac{\left|\mathbf{p}^H\,\hat{\mathbf{S}}_n^{-1}\,\mathbf{z}\right|^2}{\mathbf{p}^H\,\hat{\mathbf{S}}_n^{-1}\,\mathbf{p}} \underset{H_0}{\overset{H_1}{\gtrless}} \lambda_{AMF}$:

$$P_{fa} = \ _2F_1\left(n-m+1, n-m+2; n+1; -\frac{\lambda_{AMF}}{n}\right) ,$$

- Adaptive Kelly Filter *[Kelly 86]*: $\Lambda_{Kelly}(\mathbf{z}) = \dfrac{\left|\mathbf{p}^H\,\hat{\mathbf{S}}_n^{-1}\,\mathbf{z}\right|^2}{\left(\mathbf{p}^H\,\hat{\mathbf{S}}_n^{-1}\,\mathbf{p}\right)\,\left(n+\mathbf{z}^H\,\hat{\mathbf{S}}_n^{-1}\,\mathbf{z}\right)} \underset{H_0}{\overset{H_1}{\gtrless}} \lambda_{Kelly}$:

$$P_{fa} = \left(\frac{1}{\lambda_{Kelly}} - 1\right)^{n+1-m} ,$$

- Adaptive Normalized Matched Filter *[Scharf 94]*: $\Lambda_{ANMF}(\mathbf{z}) = \dfrac{\left|\mathbf{p}^H\,\hat{\mathbf{S}}_n^{-1}\,\mathbf{z}\right|^2}{\left(\mathbf{p}^H\,\hat{\mathbf{S}}_n^{-1}\,\mathbf{p}\right)\,\left(\mathbf{z}^H\,\hat{\mathbf{S}}_n^{-1}\,\mathbf{z}\right)} \underset{H_0}{\overset{H_1}{\gtrless}} \lambda_{ANMF}$:

$$P_{fa} = (1-\lambda_{ANMF})^{n-m+1}\ {}_2F_1\left(n-m+2, n-m+1; n+1; \lambda_{ANMF}\right) .$$

Examples of Gaussian Hypothesis Failure

High Resolution Radars

- Small number of scatterers in the cell under test - Varying number of scatterers from cell to cell - *Central Limit Theorem* non valid $\Rightarrow$ non-Gaussianity
- No validity of conventional tools based on Gaussian statistics [*Farina 87*, *Ovarlez 96*, Thesis *Jay 02*].

Low-Grazing angles Illumination Radar

- Microshadowing $\Rightarrow$ impulsive clutter [*Billingsley 93*],
- Transitions of clutter areas, heterogeneity of spatial area under test $\Rightarrow$ difficulty to set up the detection test λ_{opt} and the Probability of False Alarm depending on the area [*Ovarlez 95*].

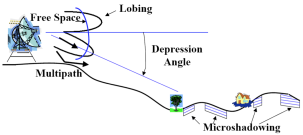

Low-Grazing angle surveillance

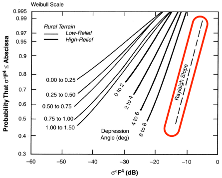

Non-Gaussian behavior

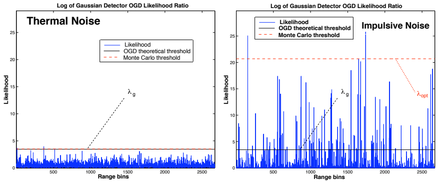

False Alarm regulation problem

Examples of Gaussian Hypothesis Failure

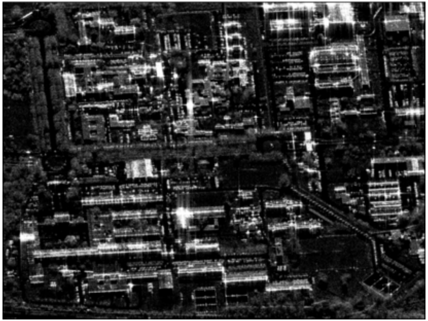

- The SAR images are more and more complex, detailed, heterogeneous. The spatial statistic of SAR images is not at all Gaussian,
- In polarimetry research field, almost all Non-Coherent Polarimetric Decomposition and classification techniques *[Lee and Pottier 09]* are generally based on conventional covariance matrix estimate (covariance or coherency matrix), typically the Sample Covariance Matrix (SCM),
- All these techniques may give very different results when using another estimates *[Formont 12]* that may fit better to the reality! Are they more physically valid? Which one to choose?

Examples of Gaussian Hypothesis Failure

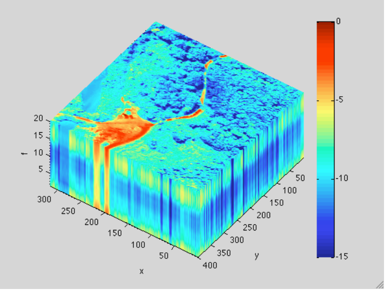

DSO data 2010

RXD CDF

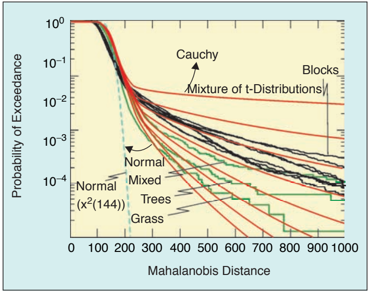

[Manolakis 2002]

- Anomaly Detection (e.g. RXD *[Reed and Yu 90]*) in Hyperspectral Images: detection of all that is different from the background (Mahalanobis distance) - Regulation of False Alarm. Application to radiance images.
- Detection of targets in Hyperspectral Images: To detect (GLRT) targets (characterized by a given spectral signature p) - Regulation of False Alarm. Application to reflectance images (after some atmospheric corrections).

Plan

Going to Robust Adaptive Detection

Generally, some parameters (*e.g.* second order statistic $\mathbf{\Sigma}$) are unknown and cannot be estimated through Gaussian methodology

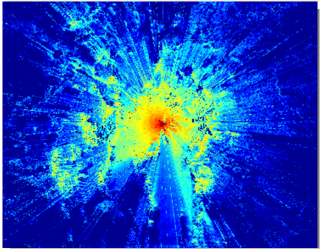

$\Rightarrow$ Robust Covariance Matrix Estimation

Requirements:

- Background modeling: SIRV (K-distribution, Weibull, etc.), CES (Multidimensional Generalized Gaussian Distributions, etc.),
- Estimation procedure: ML-based approaches, *M*-estimation, LS-based methods, etc.
- Adaptive detectors derivation and adaptive performance evaluation.

Modeling the Background

Complex Elliptically Symmetric (CES) distributions:

Let $\mathbf{z}$ be a complex circular random vector of length m. $\mathbf{z}$ has a Complex Elliptically Symmetric distribution ($CE\left(\boldsymbol{\mu}, \boldsymbol{\Sigma}, g_{\mathbf{z}}\right)$) if its PDF is *[Kelker 70, Frahm 04, Ollila 12]*:

$$g_{\mathbf{z}}(\mathbf{z}) = \pi^{-m}\, |\boldsymbol{\Sigma}|^{-1}\, h_z\left((\mathbf{z}-\boldsymbol{\mu})^H\, \boldsymbol{\Sigma}^{-1}\, (\mathbf{z}-\boldsymbol{\mu})\right),$$

where $h_z : [0,\infty) \to [0,\infty)$ is the density generator, where $\boldsymbol{\mu}$ is the statistical mean (generally known or $= \mathbf{0}_m$) and $\boldsymbol{\Sigma}$ is the scatter matrix. In general, $E\left[\mathbf{z}\,\mathbf{z}^H\right] = \alpha\,\boldsymbol{\Sigma}$ where α is known.

- **Large class of distributions**: Gaussian ($h_z(z) = \exp(-z)$), SIRV, MGGD ($h_z(z) = \exp\left(-z^{\alpha}\right)$), etc. **Validated through several experimentations** [*Billingsley 93, Ovarlez 95*],
- **Closed under affine transformations** (e.g. matched filter),
- **Stochastic representation theorem**: $\boxed{\mathbf{z} =_d \boldsymbol{\mu} + \mathcal{R}\,\mathbf{A}\,\mathbf{u}^{(k)}}$,

  where $\mathcal{R} \geq 0$, independent of $\mathbf{u}^{(k)}$ and $\boldsymbol{\Sigma} = \mathbf{A}\,\mathbf{A}^H$ is a factorization of $\boldsymbol{\Sigma}$, where $\mathbf{A} \in \mathbb{C}^{m\times k}$ with $k = \mathrm{rank}(\boldsymbol{\Sigma})$.

Modeling the Background

Spherically Invariant Random Vector: a CES subclass

The m-vector $\mathbf{z}$ is a complex Spherically Invariant Random Vector *[Yao 73, Jay 02]* if its PDF can be put in the following form:

$$g_{\mathbf{z}}(\mathbf{z}) = \frac{1}{\pi^m \, |\boldsymbol{\Sigma}|} \int_0^{\infty} \frac{1}{\tau^m} \exp\left(\frac{(\mathbf{z}-\boldsymbol{\mu})^H \, \boldsymbol{\Sigma}^{-1} \, (\mathbf{z}-\boldsymbol{\mu})}{\tau} \right) p_\tau(\tau) \, d\tau \, , \tag{1}$$

where $p_\tau : [0, \infty) \to [0, \infty)$ is the texture generator.

- **Large class of distributions**: Gaussian ($p_\tau(\tau) = \delta(\tau - 1)$), K-distribution ($p_\tau$ gamma), Weibull (no closed form), Student-t (p_τ inverse gamma), etc.
- Main Gaussian Kernel: closed under affine transformations,
- The texture random scalar τ is modeling the variation of the power of the Gaussian vector $\mathbf{x}$ along his support (e.g. heterogeneity of the noise along range bins, time, spatial domain, etc.),
- Exploitation of the spectral information using the covariance matrix (*scatter matrix*) $\boldsymbol{\Sigma}$,
- **Stochastic representation theorem**: $\boxed{\mathbf{z} =_d \boldsymbol{\mu} + \sqrt{\tau}\,\mathbf{A}\,\mathbf{x}}$, where $\tau \geq 0$ is the texture, independent of $\mathbf{x}$ and $\mathbf{x} \sim \mathcal{CN}\left(\mathbf{0}_m, \boldsymbol{\Sigma}\right)$.

Estimating the Covariance/Scatter Matrix: Conventional Estimators

Assuming n available SIRV secondary data $\mathbf{z}_k = \sqrt{\tau_k}\,\mathbf{x_k}$ where $\mathbf{x}_k \sim \mathcal{CN}(\mathbf{0}_m, \mathbf{\Sigma})$ and where τ_k scalar random variable.

- The **Sample Covariance Matrix** (SCM) may be a poor estimate of the Elliptical/SIRV Scatter/Covariance Matrix because of the texture contamination:

$$\hat{\mathbf{S}}_n = \frac{1}{n}\sum_{k=1}^{n} \mathbf{z}_k\,\mathbf{z}_k^H = \frac{1}{n}\sum_{k=1}^{n} \tau_k\,\mathbf{x}_k\,\mathbf{x}_k^H \neq \frac{1}{n}\sum_{k=1}^{n} \mathbf{x}_k\,\mathbf{x}_k^H\,,$$

- The **Normalized Sample Covariance Matrix** (NSCM) may be a good candidate of the Elliptical SIRV Scatter/Covariance Matrix:

$$\hat{\mathbf{\Sigma}}_{NSCM} = \frac{1}{n}\sum_{k=1}^{n} \frac{\mathbf{z}_k\,\mathbf{z}_k^H}{\mathbf{z}_k^H\,\mathbf{z}_k} = \frac{1}{n}\sum_{k=1}^{n} \frac{\mathbf{x}_k\,\mathbf{x}_k^H}{\mathbf{x}_k^H\,\mathbf{x}_k}\,,$$

  This estimate does not depend on the texture τ_k but it is biased and share the same eigenvectors but have different eigenvalues, with the same ordering *[Bausson 07]*.

Estimating the Covariance/Scatter Matrix

M-estimators:

Let $(\mathbf{z}_1, \ldots, \mathbf{z}_n)$ be a n-sample $\sim CE_m(\mathbf{0}_m, \mathbf{\Sigma}, g_z)$ (Secondary data).

PDF $g_z(.)$ specified: *MaximumLikelihood*-estimator of $\mathbf{\Sigma}$: $\widehat{\mathbf{\Sigma}} = \dfrac{1}{n}\displaystyle\sum_{i=1}^{n} \dfrac{-g_z'\left(\mathbf{z}_i^H \widehat{\mathbf{\Sigma}}^{-1} \mathbf{z}_i\right)}{g_z\left(\mathbf{z}_i^H \widehat{\mathbf{\Sigma}}^{-1} \mathbf{z}_i\right)} \mathbf{z}_i\, \mathbf{z}_i^H$,

PDF $g_z(.)$ not specified: *M*-estimator of $\mathbf{\Sigma}$: $\widehat{\mathbf{\Sigma}} = \dfrac{1}{n}\displaystyle\sum_{i=1}^{n} u\left(\mathbf{z}_i^H \widehat{\mathbf{\Sigma}}^{-1} \mathbf{z}_i\right) \mathbf{z}_i\, \mathbf{z}_i^H$,

[Kent et al. 91, Maronna 06, Pascal et al. 08, Mahot et al. 13]

- Existence, Uniqueness, Asymptotic Properties,
- Convergence of the recursive algorithm, etc.
- Several PhD ONERA thesis: E. Jay 02, F. Pascal 06, M. Mahot 12, E. Terreaux 18.

Examples of M-Estimators

SCM:

$u(r) = 1$

Huber's M-estimator:

$$u(r) = \begin{cases} K/e \text{ if } r <= e \\ K/r \text{ if } r > e \end{cases}$$

Tyler:

$$u(r) = \frac{m}{r}$$

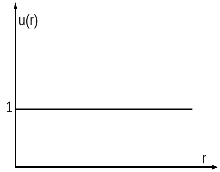

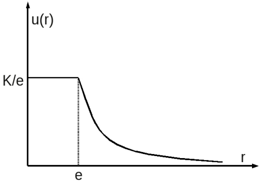

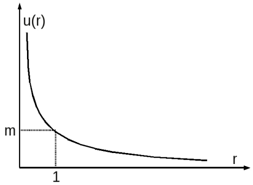

- Huber = mix between SCM and Tyler *[Huber 64]*,
- Tyler and SCM are “not" (theoretically) M-estimators,
- Tyler is the most robust while SCM is the most efficient.

Estimating the Covariance Matrix: Tyler's M-Estimators

Let $(\mathbf{z}_1, \dots, \mathbf{z}_n)$ be a n-sample $\sim CE_m\left(\mathbf{0}_m, \mathbf{\Sigma}, g_{\mathbf{z}(.)}\right)$ (Secondary data).

Tyler Estimator (*[Tyler 87, Pascal 08]*)

$$\widehat{\mathbf{\Sigma}}_{FPE} = \frac{m}{n} \sum_{k=1}^{n} \frac{\mathbf{z}_k\, \mathbf{z}_k^H}{\mathbf{z}_k^H\, \widehat{\mathbf{\Sigma}}_{FPE}^{-1}\, \mathbf{z}_k}.$$

- The Tyler M-estimator does not depend on the texture (SIRV or CES distributions),
- Convergence of the algorithm: $\widehat{\mathbf{\Sigma}}_{n+1} = f\left(\widehat{\mathbf{\Sigma}}_n\right)$ with $f(\widehat{\mathbf{\Sigma}}) = \dfrac{m}{n} \displaystyle\sum_{k=1}^{n} \frac{\mathbf{z}_k\, \mathbf{z}_k^H}{\mathbf{z}_k^H\, \widehat{\mathbf{\Sigma}}^{-1}\, \mathbf{z}_k}$ and $\widehat{\mathbf{\Sigma}}_0 = \mathbf{I}_m$.

  Existence, Uniqueness,
- True Maximum Likelihood Estimate when considering textures $\{\tau_k\}_{k\in[1,n]}$ as unknown deterministic parameters.
- Known asymptotic behavior: **Any M-estimator behaves exactly as SCM but with σ_1 more more secondary data ($\sigma_1 = (m+1)/m$ times more for Tyler)**: It implies that SCM can be simply replaced by any M-estimate in previous detectors without changing performance in Gaussian case (finite distance).

CES distribution $\Rightarrow$ two-step GLRT ANMF

Adaptive Normalized Matched Filter detector

$$H(\widehat{\boldsymbol{\Sigma}}) = \Lambda_{ANMF}(\mathbf{z}, \widehat{\boldsymbol{\Sigma}}) = \frac{\left|\mathbf{p}^H\ \widehat{\boldsymbol{\Sigma}}^{-1}\ \mathbf{z}\right|^2}{\left(\mathbf{p}^H\,\widehat{\boldsymbol{\Sigma}}^{-1}\,\mathbf{p}\right)\ \left(\mathbf{z}^H\,\widehat{\boldsymbol{\Sigma}}^{-1}\,\mathbf{z}\right)} \underset{H_0}{\overset{H_1}{\gtrless}} \lambda_{ANMF}\,,$$

where $\widehat{\boldsymbol{\Sigma}}$ stands for any M-estimators *[Conte 95, Kraut 99]*.

- The ANMF is **scale-invariant (homogeneous of degree 0)**, i.e.
  $\forall \alpha, \beta \in \mathbb{R}\,,\ \Lambda_{ANMF}(\alpha\,\mathbf{z}, \beta\,\widehat{\boldsymbol{\Sigma}}) = \Lambda_{ANMF}(\mathbf{z}, \widehat{\boldsymbol{\Sigma}})$.
- Its **asymptotic distribution** (conditionally to $\mathbf{z}$!) is known *[Pascal 15, Ovarlez 15]*.

$$\sqrt{n}\,\left(H\left(\widehat{\boldsymbol{\Sigma}}\right) - H(\boldsymbol{\Sigma})\right) \xrightarrow{d} \mathcal{CN}\left(0, 2\,\sigma_1\,H(\boldsymbol{\Sigma})\,\left(H\left(\boldsymbol{\Sigma}\right) - 1\right)^2\right)\,.$$

$$\text{Recall for SCM:}\sqrt{n}\,\left(H\left(\widehat{\mathbf{S}}\right) - H(\boldsymbol{\Sigma})\right) \xrightarrow{d} \mathcal{CN}\left(0,\,2\,H(\boldsymbol{\Sigma})\,\left(H\left(\boldsymbol{\Sigma}\right) - 1\right)^2\right)\,.$$

- **It is CFAR w.r.t the covariance/scatter matrix,**
- **It is CFAR w.r.t the texture.**

Illustrations of the Result on the ANMF

- $\Lambda = \text{var}\left(H(\widehat{\boldsymbol{\Sigma}}) - H(\boldsymbol{\Sigma})\right)$. Here $\widehat{\boldsymbol{\Sigma}}$ = complex Huber's *M*-estimator.
- Figure 1: Gaussian context, here $\sigma_1 = 1.066$.
- Figure 2: K-distributed clutter (shape parameter: $\nu = 0.1$ and 0.01).

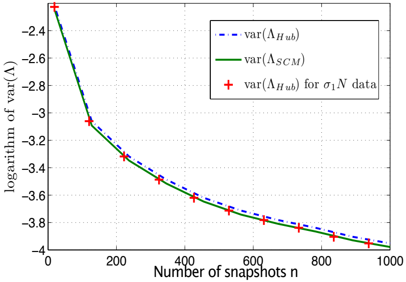

Validation of theorem (even for small *n*)

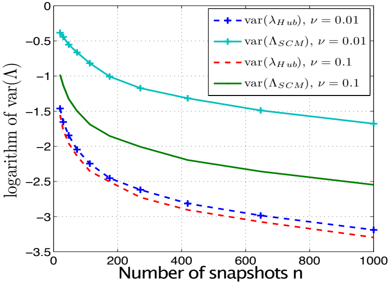

Interest of the *M*-estimators

Performances are slightly the same in Gaussian case but are clearly better in non-Gaussian case.

Illustrations of the Result on P_{fa}

- Figure 1: Gaussian context :

$$P_{fa} = (1-\lambda_{ANMF})^{n-m+1}\ {}_2F_1\left(n-m+2, n-m+1; n+1; \lambda_{ANMF}\right) .$$

- Figure 2: K-distributed clutter (shape parameter: $\nu = 0.1$), here $\sigma_1 = 1.066$:

$$P_{fa} = (1-\lambda_{ANMF})^{n/\sigma_1-m+1}\ {}_2F_1\left(n/\sigma_1-m+2, n/\sigma_1-m+1; n/\sigma_1+1; \lambda_{ANMF}\right) .$$

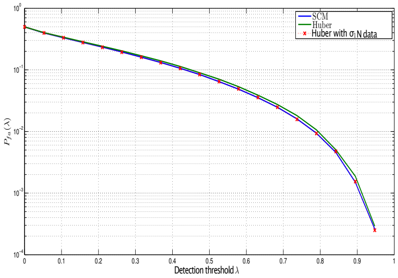

Validation of theorem (even for small n)

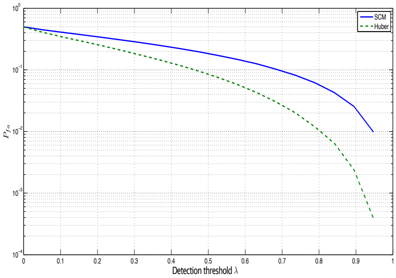

Interest of the M-estimators for False Alarm regulation

ONERA THE FRENCH AEROSPACE LAB

Illustration of the ANMF CFAR Properties For CES Noise

False Alarm regulation for ANMF built with Tyler's estimate

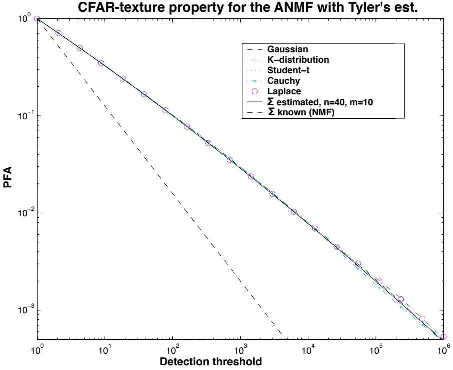

(a) CFAR-texture

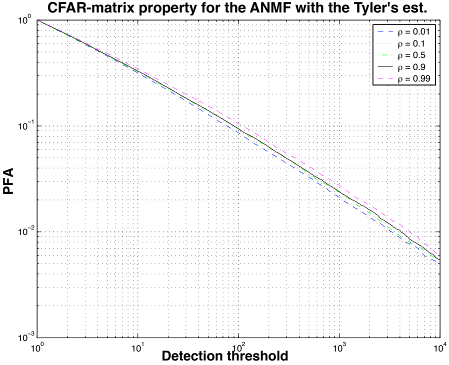

(b) CFAR-matrix

Figure: Illustration of the CFAR properties of the ANMF built with the Tyler's estimator, for a Toeplitz CM whose (i, j)-entries are $\rho^{|i-j|}$.

Properties of ANMF-Tyler Detector on Clutter Transitions

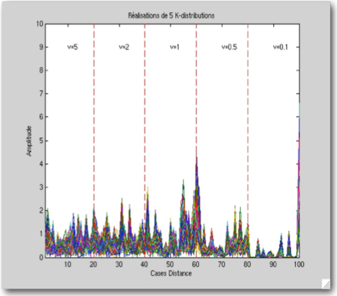

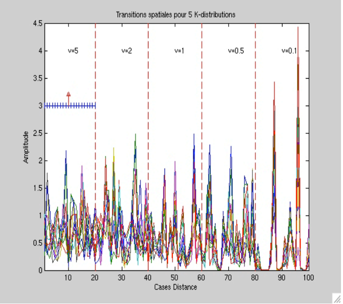

Play/Pause

- K-distributed clutter transitions: from Gaussian to impulsive noise,
- Estimation of the covariance matrix onto a range bins sliding window.

Properties of ANMF-Tyler Detector on Clutter Transitions

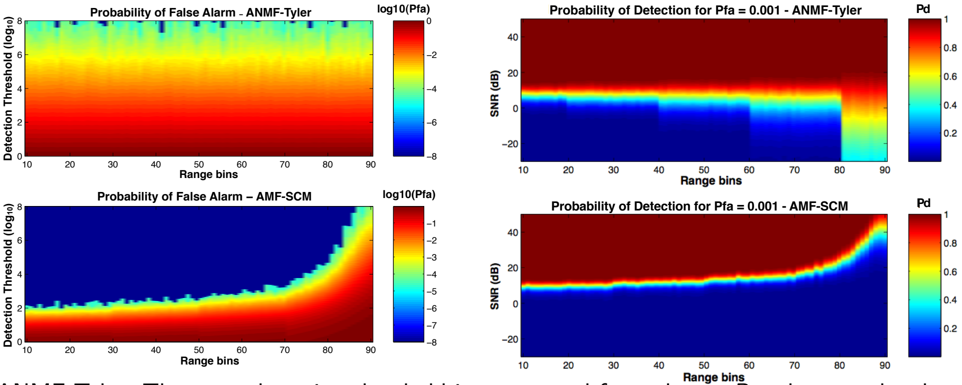

- ANMF-Tyler: The same detection threshold is guaranteed for a chosen P_{fa} whatever the clutter area,
- ANMF-Tyler: Performance in terms of detection is kept for moderate non-Gaussian clutter and improved for spiky clutter.

Plan

False Alarm Regulation on THALES Ground Clutter

Data Description

- "Range-azimuth" map from ground clutter data collected by a radar from THALES Air Defense, placed 13 meters above ground and illuminating area at low grazing angle.
- Ground clutter complex echoes collected in 868 range bins for 70 different azimuth angles and for $m = 8$ pulses.

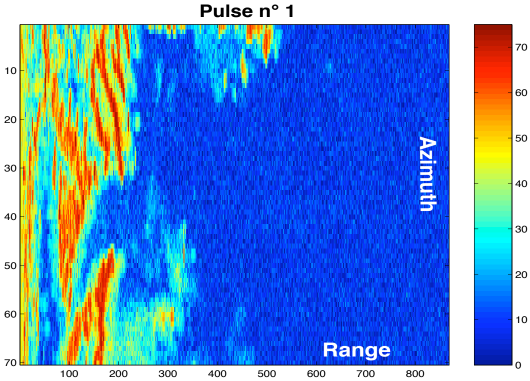

False Alarm Regulation on THALES Ground Clutter

Data processing

- Rectangular CFAR mask 5×5 for $0 \leq k \leq m$ different steering vectors $\mathbf{p}_k$.

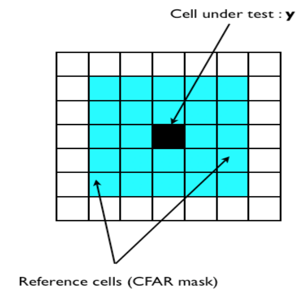

$$\mathbf{p}_k = \begin{pmatrix} 1 \\ \exp\left(\frac{2i\pi(k-1)}{m}\right) \\ \exp\left(\frac{2i\pi(k-1)2}{m}\right) \\ \vdots \\ \exp\left(\frac{2i\pi(k-1)(m-1)}{m}\right) \end{pmatrix}$$

- For each $\mathbf{z}$, computation of associated detectors $\Lambda_{ANMF}(\widehat{\mathbf{\Sigma}}_{Tyler})$ and $\Lambda_{ANMF}(\widehat{\mathbf{\Sigma}}_{NSCM})$
- Mask moving all over the map.

False Alarm Regulation on THALES Ground Clutter

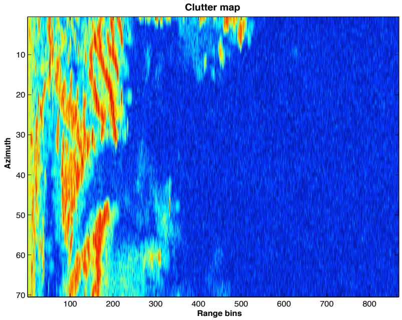

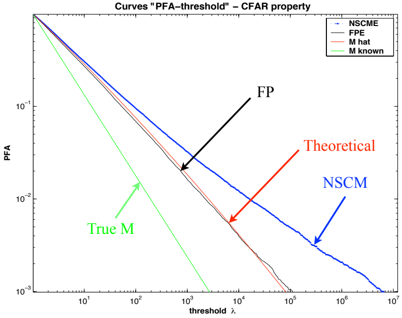

Azimut/range bins map | **Relationship "P_{fa}-threshold"**

Figure: ANMF with Tyler's M-estimate - False alarm regulation for $\mathbf{p}_0 = (1 \dots 1)^T$.

Black curve fits red curve until $PFA = 10^{-3}$ *[Ovarlez et al. 16]*.

False Alarm Regulation on THALES Ground Clutter

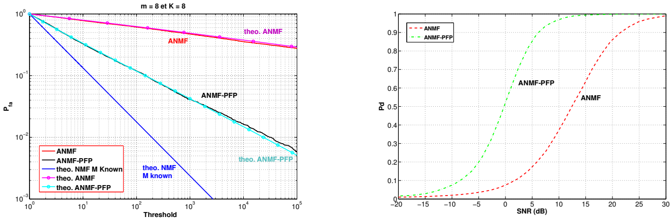

Persymmetric Tyler-ANMF and Tyler ANMF on THALES dataset - $m = 8$, $n = 8$

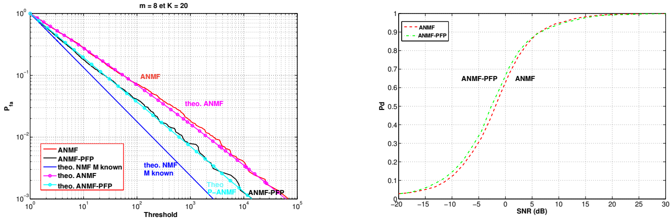

Persymmetric Tyler-ANMF and Tyler ANMF on THALES dataset - $m = 8$, $n = 20$

Detection Performance on THALES Sea Clutter

Non-Stationary and Heterogeneous THALES Sea clutter

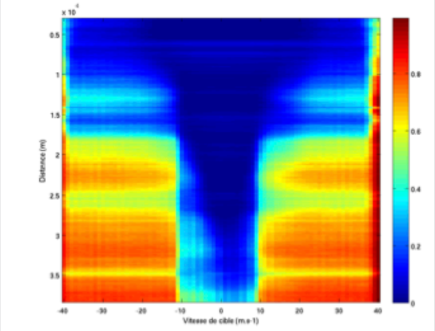

X Detector on Dieppe sea clutter

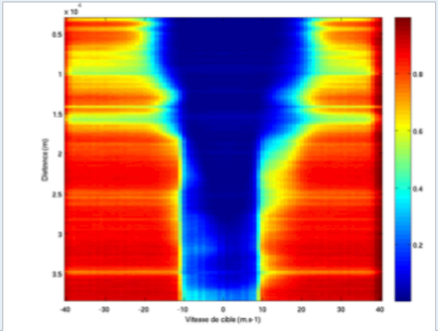

ANMF-FP Detector on Dieppe sea clutter

Detection Performance on Simulated Data

Spatially and Spectrally Heterogeneous Strong Clutter

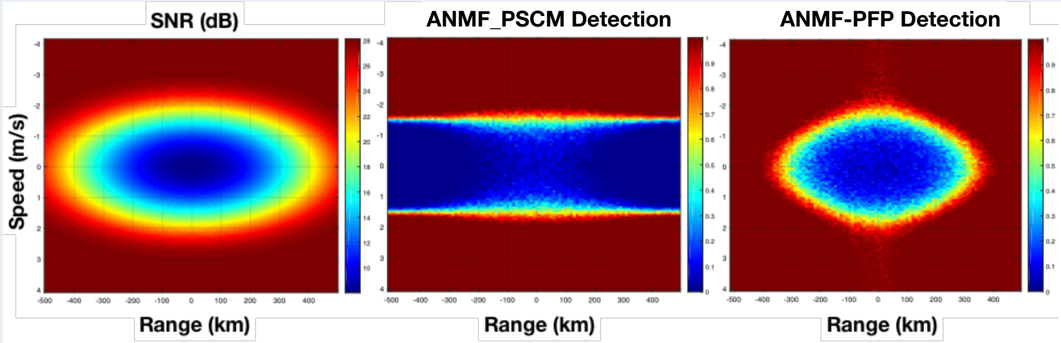

Detection Performance on STAP Data

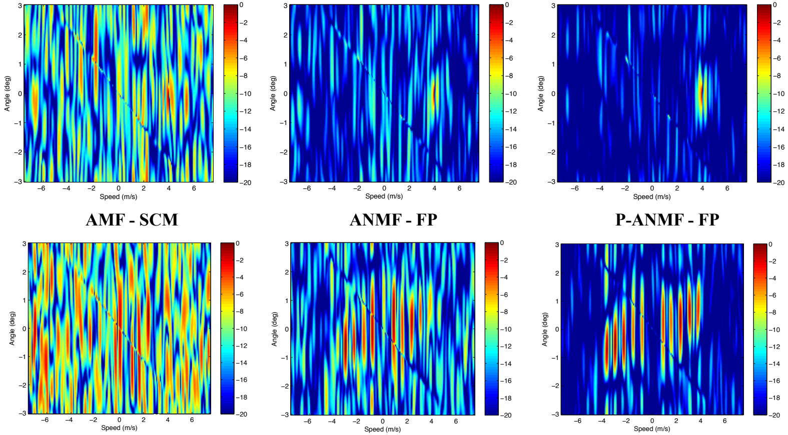

Figure: Doppler-angle map for the range bin 255 with $n = 404$ secondary data, $m = 256$ *[Pailloux 10]*

Detection Performance on SAR Image

Analysis of Performance

- Evaluation the CFAR property of the AMF and ANMF detectors,
- Comparison of the target detection performance between AMF and ANMF.

Dataset from SANDIA National Laboratories

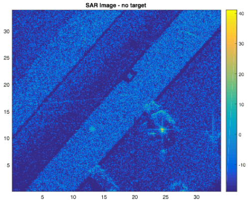

Left: Original SAR Image without target. Right: SAR image with specific embedded target.

Artificial embedded target

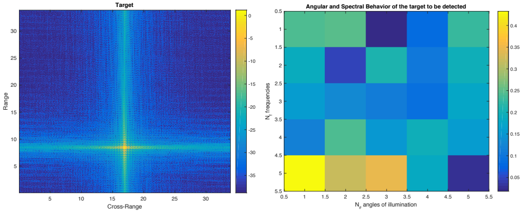

Left: SAR Image of the target. Right: True target response $\mathbf{p}$ in angular and spectral spaces ($N_\theta = 5$ sub-looks, $N_f = 5$ sub-bands).

Detection Performance on SAR Image

Perfect PFA regulation with ANMF-Tyler but poor PFA regulation for AMF-SCM

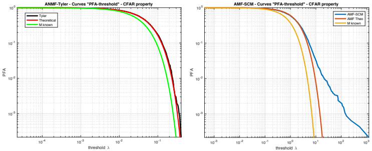

Left: FA Regulation with ANMF-Tyler. Right: FA Regulation with AMF-SCM. $N_\theta = 5$, $N_f = 5$, $K = 88$.

Better target detection for ANMF-Tyler *[Ovarlez 17, Mian 19]*

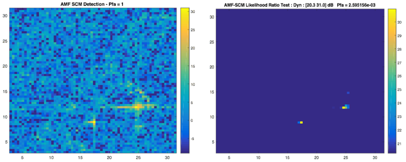

Left: Full AMF-SCM detection test, $P_{fa} = 1$. Right: AMF-SCM detection test, $P_{fa} = 2.6\,10^{-3}$.

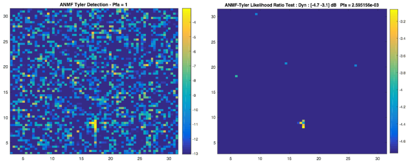

Left: ANMF-Tyler detection test, $P_{fa} = 1$. Right: ANMF-Tyler detection test, $P_{fa} = 2.6\,10^{-3}$.

Hyperspectral Imaging

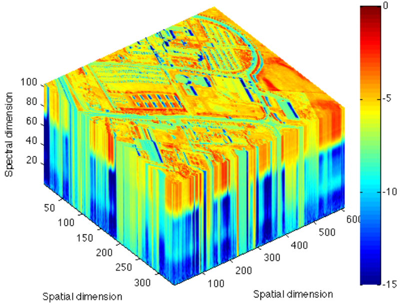

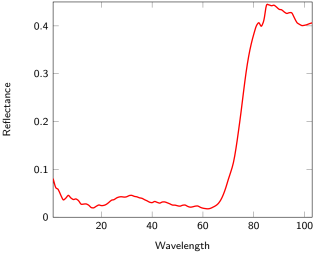

- **Anomaly Detection**
  To detect all that is "different" from the background (Mahalanobis distance) - No information about the targets of interest available *[Frontera 16]*.
- **"Pure" Detection**
  To detect targets characterized by a given spectral signature **p** - Regulation of False Alarm *[Ovarlez 11, Frontera 17]*.

Hyperspectral Imaging

ANMF and M-estimates for Hyperspectral target detection *[Frontera 14]*

$$\Lambda(\mathbf{c}) = \frac{\left|\mathbf{p}^H \widehat{\boldsymbol{\Sigma}}^{-1} (\mathbf{c} - \hat{\mu})\right|^2}{(\mathbf{p}^H \widehat{\boldsymbol{\Sigma}}^{-1} \mathbf{p}) \left((\mathbf{c} - \hat{\mu})^H \widehat{\boldsymbol{\Sigma}}^{-1} (\mathbf{c} - \hat{\mu})\right)} \underset{H_0}{\overset{H_1}{\gtrless}} \lambda$$

$$P_{fa} = (1-\lambda)^{\frac{n-1}{\sigma_1} - m + 1} \, {}_2F_1\left(\frac{n-1}{\sigma_1} - m + 2, \frac{n-1}{\sigma_1} - m + 1; \frac{n-1}{\sigma_1} - 1; \lambda\right), \text{ where } \sigma_1 = (m+1)/m\,.$$

- This two-step GLRT test is homogeneous of degree 0: it is independent of any particular Elliptical distribution: CFAR texture and CFAR Matrix properties,
- Under homogeneous Gaussian region, it reaches the same performance than those of the detector built with the SCM estimate.

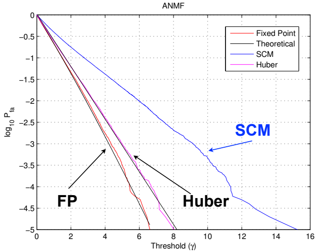

Hyperspectral Imaging

Non-Gaussian region

Original data set

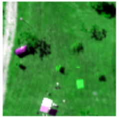

<u>Extracted region :</u>

- 100 x 100 pixels,
- 5 bands,
- Sliding Window: 19x19

Selected bands

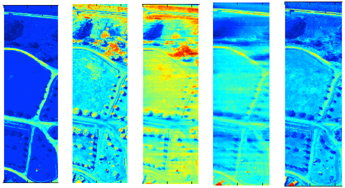

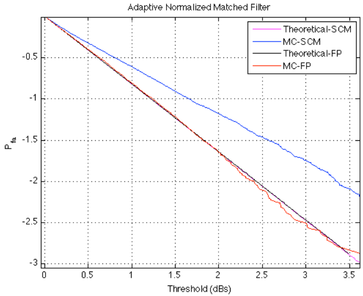

Hyperspectral Imaging (HSI)

GLRT RX Anomaly Detector: Mahalanobis Distance *[Reed 90]*

Binary Hypotheses test: $\begin{cases} H_0 \;:\; \mathbf{c} = \mathbf{b} & \mathbf{c}_1, \dots, \mathbf{c}_n \\ H_1 \;:\; \mathbf{c} = A\,\mathbf{p} + \mathbf{b} & \mathbf{c}_1, \dots, \mathbf{c}_n \end{cases}$ where $\mathbf{b} \sim \mathcal{CN}(\mathbf{0}_m, \boldsymbol{\Sigma})$ and $\mathbf{c}_i \sim \mathcal{CN}(\mathbf{0}_m, \boldsymbol{\Sigma})$, A known and $\mathbf{p}$ unknown

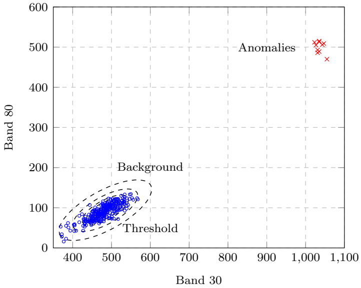

denoting $\hat{\mu} = \frac{1}{n}\sum_{i=1}^{n} c_i$

$$RXD_{SCM}(\mathbf{c}) = (\mathbf{c} - \hat{\mu})^H\, \hat{\mathbf{S}}_n^{-1}\, (\mathbf{c} - \hat{\mu}) \underset{H_0}{\overset{H_1}{\gtrless}} \lambda$$

(Hotelling T^2 distributed)

$$\frac{n-m}{m\,(n+1)} RXD_{SCM}(\mathbf{c}) \sim F_{m,n-m}$$

- Derived and valid only under Gaussian hypotheses,
- Its false alarm rate is independent of the covariance matrix: CFAR-matrix property in homogeneous Gaussian data.

Hyperspectral Imaging

Extended GLRT RX Anomaly Detector: Mahalanobis Distance *[Frontera 14]*

Binary Hypotheses test: $\begin{cases} H_0 & : \quad \mathbf{c} = \mathbf{b} \qquad\qquad \mathbf{c}_1, \dots, \mathbf{c}_n \\ H_1 & : \quad \mathbf{c} = A\,\mathbf{p} + \mathbf{b} \quad \mathbf{c}_1, \dots, \mathbf{c}_n \end{cases}$ where $\mathbf{b} \sim CE(\boldsymbol{\mu}, \boldsymbol{\Sigma}, g_{\mathbf{z}})$ and $\mathbf{c}_i \sim CE(\boldsymbol{\mu}, \boldsymbol{\Sigma}, g_{\mathbf{z}})$,

A known and $\mathbf{p}$ unknown

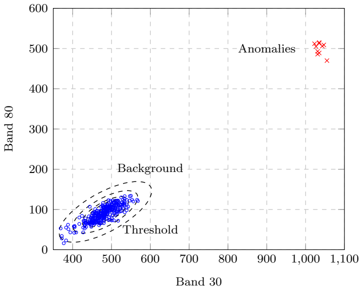

$$RXD_{M-est}(\mathbf{c}) = (\mathbf{c} - \hat{\boldsymbol{\mu}})^H\, \widehat{\boldsymbol{\Sigma}}^{-1}\, (\mathbf{c} - \hat{\boldsymbol{\mu}}) \underset{H_0}{\overset{H_1}{\gtrless}} \lambda$$

where $\widehat{\boldsymbol{\Sigma}}$ and $\hat{\boldsymbol{\mu}}$ are M-estimates of the location and scale

- Derived and valid for any Elliptical Contoured Distributions,
- Its false alarm rate unfortunately depends on texture statistic of the data.

Anomaly Detection Results on Artificial Targets

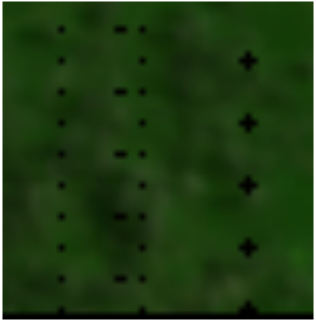

Original image (Forest Region)

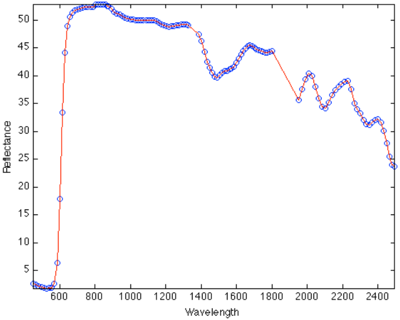

Target Spectrum

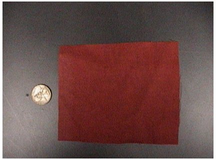

50 x 50 pixels, 126 spectral bands

Anomaly Detection Results on Artificial Targets

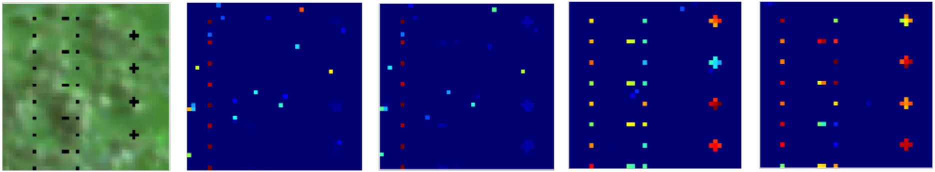

(a) Original (b) SCM (c) Shr-SCM (a) FP (b) Shr-FP

Extended Kelly AD built with conventional and robust estimates for artificial targets in real HSI ($m = 9$, $n = 80$, PFA $= 0.03$).

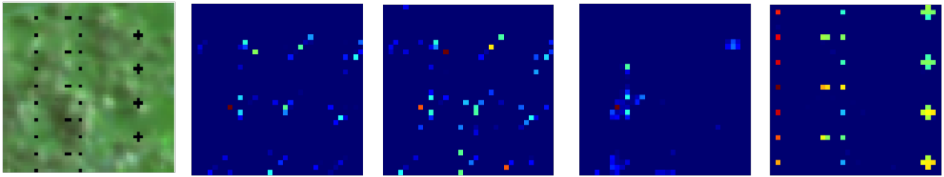

(a) Original (b) SCM (c) Shr-SCM (a) FP (b) Shr-FP

Extended Kelly AD built with conventional and robust estimates for artificial targets in real HSI ($m = 126$, $n = 288$, PFA $= 0.03$).

ONERA THE FRENCH AEROSPACE LAB

Galaxies Anomaly Detection Results on MUSE data

Problem of detecting galaxies in HS MUSE (Multi Unit Spectroscopic Explorer) data (465-930 nm)

Classical RXD

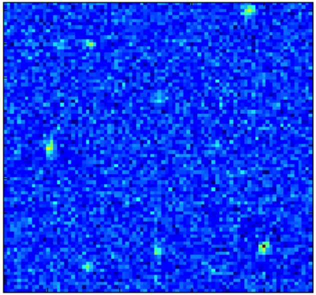

$RXD_{SCM}(\mathbf{c})$

Muse Image

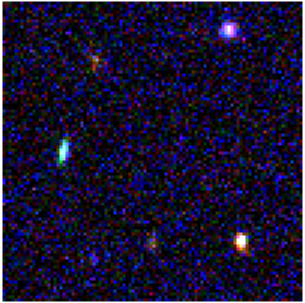

300 x 300 pixels
3578 spectral bands

Extended RXD

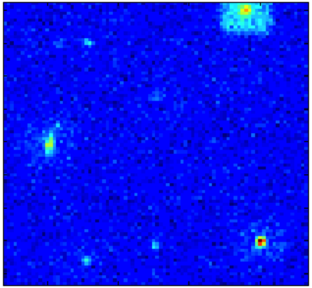

$RXD_{Tyler}(\mathbf{c})$

Better detection and False Alarm regulation with Tyler estimate (same Pfa).

Bibliography

- S. M. Kay, *Fundamentals of Statistical Signal Processing - Detection Theory*, Vol. 2, Prentice-Hall PTR, 1998.
- E. J. Kelly, An adaptive detection algorithm, *Aerospace and Electronic Systems, IEEE Transactions on*, **23**(1):115–127, 1986.
- F.C. Robey, D. R. Fuhrmann, E. J. Kelly and R. Nitzberg, A CFAR adaptive matched filter detector, *Aerospace and Electronic Systems, IEEE Transactions on*, **28**(1):208–216, 1992.
- L. L. Scharf and B. Friedlander, Matched subspace detectors, *Signal Processing, IEEE Transactions on*, **42**(8):2146–2157, 1994.
- A. Farina, A. Russo and F. Scannapieco, Radar detection in coherent Weibull clutter, *Acoustics, Speech, and Signal Processing, IEEE Transactions on*, **35**(6), June 1987.
- E. Jay, *Detection in non-Gaussian noise*, PhD thesis, University of Cergy-Pontoise / ONERA, France, 2002.
- J.-P. Ovarlez, ONERA RT 6/5275 SN, Détection en Environnement Non-Gaussien, oct. 1996.
- J.-P. Ovarlez, ONERA RT 25/5272 SY, Evaluation de la Détectabilité des Cibles Volant à Basse Altitude par des Radars Sols, mai 1995.
- J. B. Billingsley, Ground Clutter Measurements for Surface-Sited Radar, *Technical Report*, 780, MIT, February 1993.
- J.-S. Lee and E. Pottier, *Polarimetric Radar Imaging, From Basics to Applications*, CRC Press, 2009.
- P. Formont, *Statistical and Geometric Tools for the Classification of Highly Textured Polarimetric SAR Images*, PhD Thesis, Paris Saclay University / ONERA, 2012.

Bibliography

- I. Reed and X. Yu, Adaptive multiple-band CFAR detection of an optical pattern with unknown spectral distribution, *Acoustics, Speech and Signal Processing, IEEE Transactions on*, **38**(10):1760–1770, 1990.
- D. Kelker, *Distribution theory of spherical distributions and a location-scale parameter generalization*, Sankhya A 32, 1970.
- G. Frahm, *Generalized elliptical distributions: theory and applications*, PhD thesis, Universitätsbibliothek, 2004.
- E. Ollila, D. E. Tyler, V. Koivunen and H. V. Poor, Complex elliptically symmetric distributions: Survey, new results and applications, *Signal Processing, IEEE Transactions on*, **60**(11), 2012.
- K. Yao, A representation theorem and its application to spherically invariant random processes, *Information Theory, IEEE Transactions on*, **19**(2), 1973.
- S. Bausson, F. Pascal, P. Forster, J.-P. Ovarlez and P. Larzabal, First and second order moments of the normalized sample covariance matrix of spherically invariant random vectors, *IEEE Signal Processing Letters*, **14**(6):425–428, 2007.
- J. T. Kent and D. E Tyler, Redescending M-estimates of multivariate location and scatter *Annals of Statistics*, **19**(4):2102–2119, 1991.
- R. A. Maronna, D. R. Martin and J. V. Yohai, *Robust Statistics: Theory and Methods*, Wiley Series in Probability and Statistics, John Wiley & Sons, 2006.
- F. Pascal, *Détection et Estimation en Environnement Non-Gaussien*, PhD thesis, University of Nanterre / ONERA, France, 2006.
- M. Mahot, *Robust Covariance Estimation in Signal Processing*, PhD thesis, Ecole Normale de Cachan / ONERA , 2013.

Bibliography

- M. Mahot, F. Pascal, P. Forster and J.-P. Ovarlez, Asymptotic properties of robust complex covariance matrix estimates, *Signal Processing, IEEE Transactions on*, **61**(13):3348–3356, 2013.
- E. Terreaux, *Robust model order selection using Random Matrix Theory*, PhD Thesis, University Paris Saclay / ONERA, 2018.
- P. J. Huber, Robust estimation of a location parameter, *The Annals of Mathematical Statistics*, **35**(1), 1964.
- F. Pascal, Y. Chitour, J.-P. Ovarlez, P. Forster and P. Larzabal, Covariance structure maximum-likelihood estimates in compound gaussian noise: Existence and algorithm analysis, *Signal Processing, IEEE Transactions on*, **56**(1):34–48, 2008.
- D. E. Tyler, A distribution-free M-estimator of multivariate scatter, *The Annals of Statistics*, **15**(1), 1987.
- J.-P. Ovarlez, F. Pascal and A. Breloy, Asymptotic detection performance analysis of the robust adaptive normalized matched filter, *IEEE 6th International Workshop on Computational Advances in Multi-Sensor Adaptive Processing* (CAMSAP), pages 137–140, 2015.
- F. Pascal and J.-P. Ovarlez, Asymptotic properties of the robust ANMF, *IEEE International Conference on Acoustics, Speech and Signal Processing* (ICASSP), pages 2594–2598, 2015.
- G. Pailloux, *Estimation Structurée de la Matrice de Covariance et Application à la Détection Radar*, PhD thesis, University of Nanterre / ONERA, France, 2010.
- G. Pailloux, P. Forster, J.-P. Ovarlez and F. Pascal, Persymmetric adaptive radar detectors, *Aerospace and Electronic Systems, IEEE Transactions on*, **47**(4):2376–2390, 2010.
- E. Conte, M. Lops and G. Ricci, Asymptotically optimum radar detection in compound-gaussian clutter, *Aerospace and Electronic Systems, IEEE Transactions on*, **31**(2):617–625, 1995.
- S. Kraut and L. L. Scharf, The CFAR adaptive subspace detector is a scale-invariant GLRT, *Signal Processing, IEEE Transactions on*, **47**(9):2538–2541, 1999.

Bibliography

- J.-P. Ovarlez, G. Ginolhac and A. M. Atto, Multivariate linear time-frequency modeling and adaptive robust target detection in highly textured monovariate SAR image, *IEEE International Conference on Acoustics, Speech and Signal Processing* (ICASSP), pages 4029–4033, 2017.
- A. Mian, *Robust Change Detection in Time Series SAR Images*, PhD Thesis, Université de Paris Saclay / ONERA, 2019.
- A. Mian, J.-P. Ovarlez, A. M. Atto and G. Ginolhac, Design of New Wavelet Packets Adapted to High-Resolution SAR Images With an Application to Target Detection, *Geoscience and Remote Sensing, IEEE Transactions on*, **57**(6), pp.3919-3932, June 2019
- J.-P. Ovarlez, S. K. Pang, F. Pascal, V. Achard and T.K. Ng, Robust Detection using the SIRV Background Modelling for Hyperspectral Imaging, *Proc IEEE-IGARSS*, Vancouver, Canada, July 2011.
- J. Frontera-Pons, *Robust Detection and Classification for Hyperspectral Imaging*, PhD Thesis, Paris Saclay University / ONERA, 2014.
- J. Frontera-Pons, M. A. Veganzones, S. Velasco-Forero, F. Pascal, J.-P. Ovarlez, J. Chanussot, Robust Anomaly Detection in Hyperspectral Imaging, *Proc. IEEE-IGARSS*, Quebec, Canada, July 2014.
- J. Frontera-Pons, M. A. Veganzones, F. Pascal and J.-P. Ovarlez, Hyperspectral Anomaly Detectors using Robust Estimators, *Selected Topics in Applied Earth Observation and Remote Sensing (IEEE-JSTARS), IEEE Journal of*, **9**(2), pp.720-731, 2016.
- J. Frontera-Pons, F. Pascal, J.-P. Ovarlez, Adaptive Nonzero-Mean Gaussian Detection, *Geoscience and Remote Sensing, IEEE Transactions on*, **55**(2), pp.1117-1124, 2017.
- J. Frontera-Pons, J.-P. Ovarlez and F. Pascal, Robust ANMF Detection in Noncentered Impulsive Background, *IEEE Signal Processing Letters*, **24**(12), pp.1891-1895, 2017.